Progress in Organic Coatings 148 (2020) 105847

Contents lists available at ScienceDirect

Progress in Organic Coatings

journal homepage: www.elsevier.com/locate/porgcoat

Surface roughness profile and its effect on coating adhesion and corrosion protection: A review

S.G. Croll

Department of Coatings and Polymeric Materials, North Dakota State University, Fargo, ND, United States

ARTICLE INFO

Keywords:
Adhesion
Corrosion
Roughness
Mode II
Surface gradient
Developed area

ABSTRACT

Specifications for coating many forms of infrastructure and equipment include abrasive cleaning, then measurement of the surface profile and adhesion on the assumption that they are linked to long term prevention of corrosion undercutting the coating. Studies find no quantitative connection between adhesion and corrosion protection, but many believe in a link. Although corrosion is a molecular phenomenon that starts at the interface, adhesion values are measured by a device attached to the coating at some distance from the interface, so it is difficult to directly connect corrosion with adhesion. Understanding how adhesion and the spread of corrosion under the coating are influenced by surface roughness entails surface metrology, fracture mechanics, surface energy and viscoelasticity. The impact of surface roughness cannot be not determined by a simple, or single, statistical parameter for variation in substrate height variation. Conventional "pull-off" adhesion testing does not characterize coating-metal interactions that might prevent water and electrolyte causing corrosion, they must be determined otherwise. The additional surface area created by the abrasion increases the number of adhesive interactions and the local slope of the surface engages Mode II loading that increases the force that the interface can support. Both these surface attributes may also slow the spread of corrosion across the interface. In order to prevent the diffusion of water and electrolyte across the interface, a coating should form well at the interface, be tough and as hydrophobic as realistically possible.

1. Introduction

Essentially, there are two routes for corrosive species to attack a coated metal surface. One is through the thickness of the coating, which is dictated by the composition and possible defects in the body of the coating [1] where the coating acts as a barrier to water and other corrosive species. In the second case, a defect or damage to the coating exposes the metal so that water and corrosive electrolyte have direct access to the metal and can spread along the interface with the metal. A common term for this lateral spread of corrosion under the coating is "corrosion creep". There are very few quantified comparisons of the two routes [2] but in one notable case the diffusion coefficient of water through a coating was found to be 6×10^{-13} m^2/s [3] which was two orders of magnitude slower than the diffusion coefficient of sodium ions, and presumably water, along the interface between the same coating and a (smooth) metal substrate, 6.4×10^{-11} m^2/s [4]. This is an important large difference. A corrosion failure may well have had contributions from both paths, but the focus here is on the interface between coating and metal substrate.

Large infrastructure is expensive to build, maintain and repair. A structure must last a very long time and be tested in a way that gives confidence in its engineered durability. One of the crucial tests done to a coated component is to measure the adhesion of the coating to the metal because that is an indicator of coating integrity. There is a great deal of support and evidence that having a rough interfacial profile improves adhesion. Long term corrosion protection relies on the integrity of the coating so the prevailing and plausible assumption is that improving adhesion will improve the life of the corrosion protection [5]. The underlying assumption in the infrastructure industry is that strong adhesion is the principal way that a coating restricts the access and motion of corrosive species. There has been considerable difficulty connecting adhesion and corrosion protection, especially with surface roughness as the variable, for many decades [6–14]. Routinely used surface roughness parameters are the average deviation from the mean height and peak density but there are many other parameters, e.g. surface area, angularity, sharpness etc. discussed [15,16]. Evidence, both empirical and theoretical, is that the effect of surface profile is not straightforward. The purpose of this review is to uncover, from a variety of disciplines, what the connections between adhesion, corrosion protection and surface roughness might be.

Long term barrier protection of steel infrastructure requires organic polymer coatings with a thickness that is a substantial fraction of a

E-mail address: Stuart.Croll@ndsu.edu.

https://doi.org/10.1016/j.porgcoat.2020.105847
Received 21 April 2020; Received in revised form 8 June 2020; Accepted 16 June 2020
Available online 08 July 2020

millimeter. For infrastructure or large engineered equipment, the criteria for how rough the surface profile is related to the thickness of the barrier coating. Thicker coatings are supported better by the metal substrate if the metal is rougher and thus protrudes more into the polymer coating but there are limits. A very rough surface might have debris that is difficult to remove and it might be difficult to fill the deepest valleys with paint or, with a fixed rate of paint application, to cover the highest peaks with a thick enough barrier to prevent moisture and salt attacking those summits. Specifying a level of adhesion and the roughness of the surface profile is very common in applications where the primary function of the coating is to prevent corrosion for a long service life and where the requirements on appearance are not very stringent. Usually the pull-off adhesion test [17] is specified as quality control on freshly manufactured coated infrastructure parts, and again just before the structure is accepted to enter service.

A different focus exists on the connection between surface roughness and adhesion of soft polymers that are pressed onto surfaces [18]. This concerns pressure sensitive adhesives (PSA), or rubber tyres etc., where the adhesive polymer is premade and adhesive forces are largely determined by the area of contact and the viscoelastic properties of the polymer. While there are some similarities, conventional coatings are applied as liquids that then solidify and change composition and properties through reactive chemistry and solvent loss.

In other applications, coatings have stringent appearance requirements. For example, automotive coatings are usually required to be very glossy and thin (more economical and lightweight) so they must be very smooth and cannot have a highly profiled surface below them. In this and similar situations, a chemical conversion of the surface is used to inhibit corrosion and to aid adhesion but with a roughness on a scale much smaller than the coating thickness. There has been considerable research on this [19], often targeting aluminium and its alloys, and has had the additional merit of attempting to replace chromate conversion coatings. This review will not include the large amount of work that has been done on conversion coatings and the exact nature of interfacial bonds but will deal with the topology of roughened surfaces.

Metal substrates are roughened for other reasons, e.g. for optical effects or for controlling friction, and by other techniques e. g. electron beam texturing, electrical discharge texturing etc. [20]. The focus here will be on metal that is roughened to improve its adhesion and corrosion performance and the examples used here will be on abrasive-blasted steel.

In overall coating service, first the paint impinges on the surface, then it must spread over the surface, including into all the nooks and crannies in the surface profile. After cure, the coating must exhibit strong adhesion in order to be qualified for its protective purpose. In service, the coating must resist the spread of corrosion underneath the coating from any damaged site that allows corrosive salts and water to spread along the interface with the metal. The objective here is to review what is known about how a rough surface affects each of these stages, sometimes from disciplines that are not often considered in protective coatings and seek possible connections without dealing with specific coating compositions.

2. Surface profile

Images, in Fig. 1, are from scanning electron microscopy (SEM) with the 3D surface profile constructed from stereo pairs (7-degree offset) using MEX software (Bruker-Alicona) [21]. The data from these surfaces are used as examples for the discussion here. SEM provides a very large range of magnifications with a large depth of focus.

Two surfaces are shown here. They are examples from large steel pipes; at the time of abrasive-blasting the profiles were measured by industry standard practices and deemed well within specification; the coated pipeline has since performed well in service. Details of the data acquisition and measurement methods has been published separately [21], but some information is given as a basis for discussion.

In each case a line scan was done down the middle of the images above. Fig. 2 shows that profile scan from each and the statistics are given for the line profiles in Table 1. Table 2 has the parameters calculated from the whole 3D surfaces.

The line profiles, when plotted with both axes having the same scale, are not very jagged like illustrations usually used in discussions, even in standards, on surface profile. The misleading impression left by such cartoons has been noted over the years [22] but is pointed out again here. The expanded view is much more consistent with the impression made by the normal SEM images in Fig. 1 that the surface is rough but not as jagged as the upper images in Fig. 2 would suggest. In addition, overhanging features, that a coating might get under, were seldom visible in any field of view or magnification of the exemplar surfaces in Figs. 1 and 2, so the term “interlocking” which often connotes dovetailing is not an accurate description of these surfaces.

Surface profile evaluation is often done with a stylus profilometer (ASTM D7127) and may be in combination with replica tape (ASTM D4417) [10,23]. Usually, average peak height is recorded together with peak density. Other parameters often enter discussion, e.g. surface area and angularity, but may not be quantified or recorded routinely due to the limitations of the profilometer or because they are not required in the project specifications.

The most common expression for average peak height is R_a which is the arithmetic mean of the deviations, y_i, from the mean height of the surface profile over n measurement positions:

$$R_a = \frac{1}{n}\sum_{i=1}^{n} |y_i|$$

Another expression for average peak height is the root mean square, RMS, deviation, R_{rms}:

$$R_{rms} = \sqrt{\frac{1}{n}\sum_{i=1}^{n} |y_i|^2}$$

RMS height deviation is closely linked to the optical reflectance of a surface [24]. Optical profilometry has been a topic of research and used for many years [25] but such instruments are expensive and not yet as widespread as scanning electron microscopes. When viewed perpendicularly an ideal abraded metal surface would appear grey, i.e. only diffuse scattering from the surface, without glitter from specular reflections that would be from horizontal facets.

It is useful to have an expression of the lateral distribution of features in the roughness profile. Peak density is peaks/length measured with a stylus profilometer or peaks/area seen on replica tape. Any profile feature larger than the instrument noise (or uncertainty) that extends from below the mean height, reaches a summit, and then returns below the mean can be considered a peak.

In many cases “roughness”, r, is taken as the ratio of surface area (which depends on the resolution of the imaging device) developed by the roughening process to the area that the measurement spans. It cannot be measured accurately when a simple stylus or replica tape is used. This parameter is often given other names, e.g. rugosity, surface area index, Wentzel roughness.

Skewness and Kurtosis are sometimes calculated (for large n):

$$Skewness = \frac{{}^{1}/_{n}\sum_{i=1}^{n} y_i^3}{(std.\ dev.)^3} \quad Kurtosis = \frac{{}^{1}/_{n}\sum_{i=1}^{n} y_i^4}{(std.\ dev.)^4}$$

Skewness shows whether a profile is biased towards high summits or deep valleys. This is significant if there are deep valleys which may not fill with paint or there are high summits that might be difficult to cover. A surface with a Normal distribution of height has a skewness of zero. Kurtosis is even more sensitive to the profile outliers than skewness. For a Normal height distribution, Kurtosis would have a value of 3; higher values indicate a flatter distribution with many outliers; smaller Kurtosis indicates the opposite.

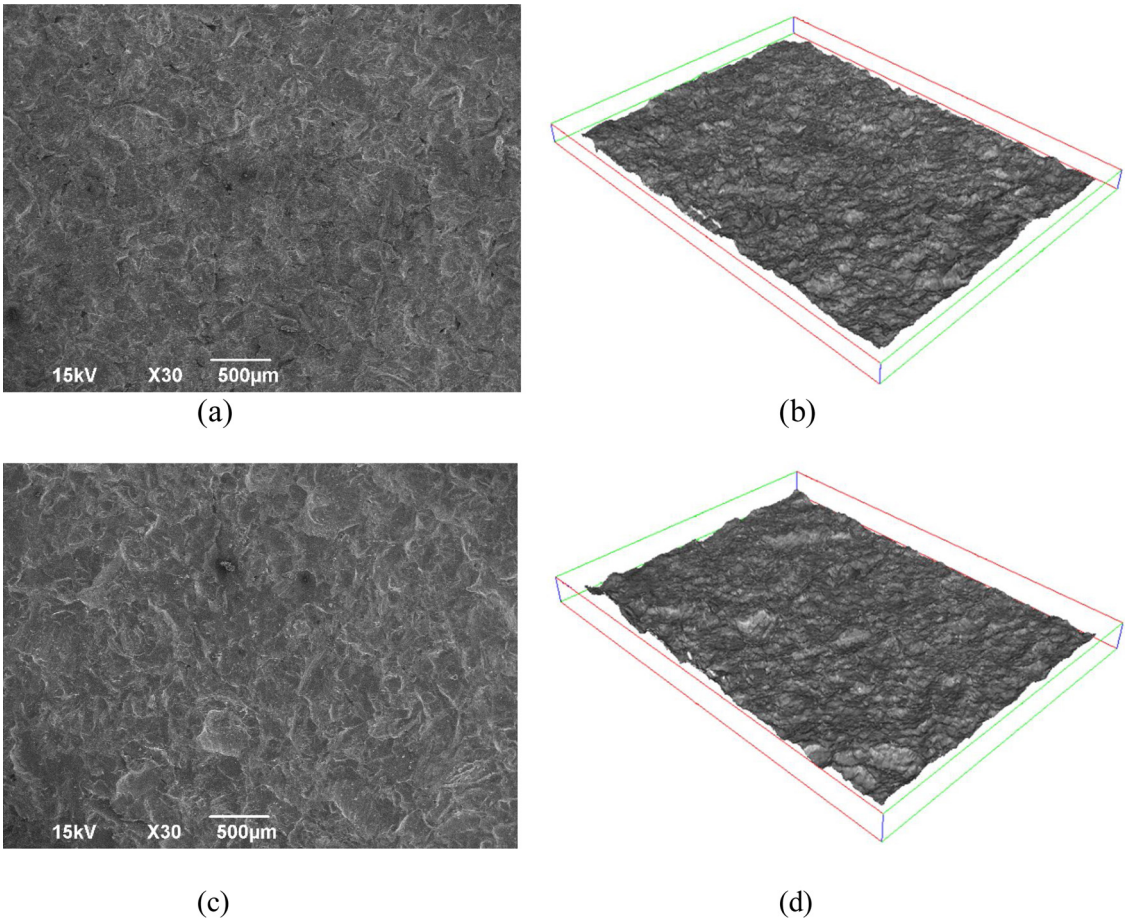

Fig. 1. Two grit blasted steel surfaces, scan area: 4.3 mm x 3.2 mm. Example 1 (field blasting, 100 grit): (a) conventional scanning electron micrograph; (b) 3D surface constructed from stereo pair. Example 2 (factory centrifugal blasting, 100 grit) (c) scanning electron micrograph; (d) 3D surface constructed from stereo pair. The depth on the box around the 3D images is 290 µm. Height variation can be seen from the profiles in Fig. 2.

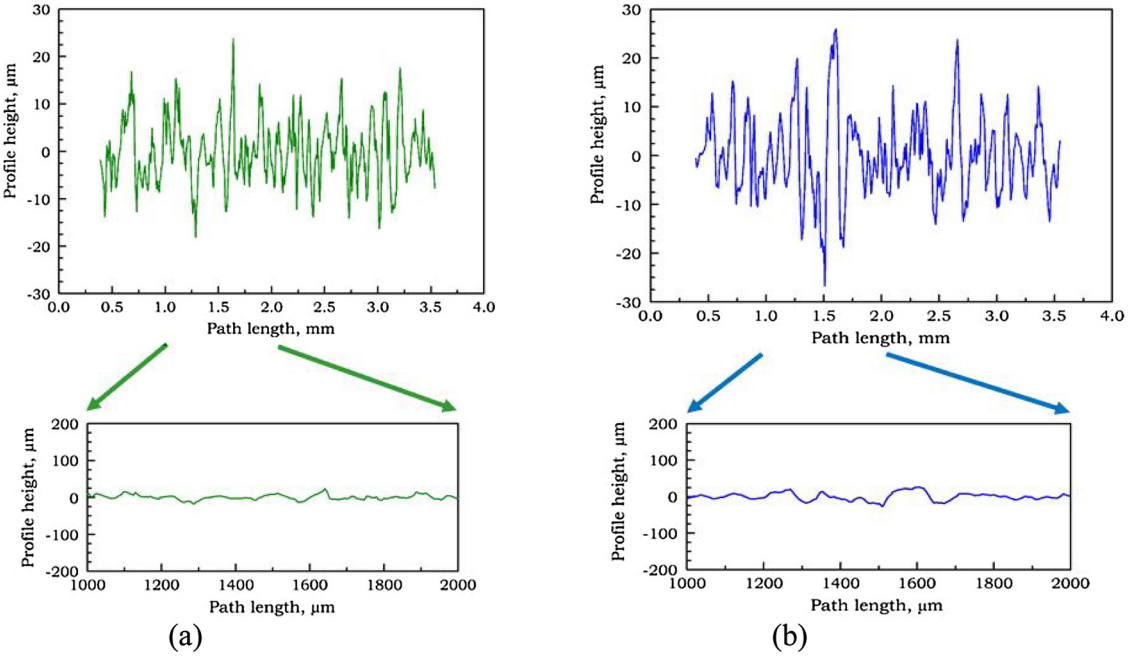

Fig. 2. Line profiles across the middle of the surfaces in Fig. 1. (a) is from example 1 and (b) is from example 2. The lower plot of each pair is an expanded view of the 1.0 to 2.0 mm part of the path, plotted so that each axis uses the same scale.

Table 1
Line profile statistics for the profiles in Fig. 2.

Example 1	Line Profile Parameter	Example 2
5.1	Average roughness, R_a μm	6.2
6.5	Root-Mean-Square roughness, R_{rms} μm	8.18
41.9	Maximum peak to valley height, R_t μm	52.7
32.5	Mean peak to valley height, R_z μm	35.5
0.17	Skewness, R_{sk}	0.38
2.96	Kurtosis, R_{ku}	3.7
0.54 (28)	Root mean square gradient (degrees)	0.53 (28)
1.26	Roughness ratio, r	1.15
1.03	Fractal Dimension, d_f	1.03

Table 2
Surface profile statistics for the 3D surfaces in Fig. 1.

Example 1	Area Parameter	Example 2
17.1	Average height, S_a, μm	17.5
21.6	Root-Mean-Square height, S_q, μm	22.9
85.9	Maximum peak height, S_p, μm,	94.0
84.9	Maximum valley depth, S_v, μm	120.2
−0.035	Skewness, S_{sk}	−0.28
3.1	Kurtosis, S_{ku}	4.18
0.80 (39)	Root mean square gradient, (degrees)	0.72 (36)
1.29	Roughness ratio, r	1.24
2.06	Fractal Dimension, d_f	2.05

Altogether, there are more than 50 parameters that may be calculated from a detailed surface scan [15,16]. Even now, there is no simple or completely satisfactory approach to characterizing a surface [26]. Instrument output and calculations usually adhere to ISO and ASME standards but may report a different set of parameters for line and surface data.

The value for roughness ratio given in Table 1 is the square of the tortuosity of the line trace. There was no calculation of the fractal dimension given in the standard output for a line profile although that parameter has been used to characterize rough surfaces. The calculation for fractal dimension of the line profiles used Richardson's dimension method [21,27] on data downloaded from the instrument. Fractal dimension, d_f, is a numerical ratio that indicates how much a line or surface is more complex than a smooth 1D or 2D figure. For idealized fractal shapes, the same degree of complexity occurs no matter how small a part of a fractal line or surface is examined so a single value of d_f can describe it from the macroscopic level down to the atomic level. In practice, no line or surface can be made consistently complex at all length scales but fractal dimension is an obvious, and possibly important, candidate parameter for describing ramified lines, shapes and surfaces [21,27–29].

Some of the discussion about these parameters will be given in the following sections, but a few observations are given here. The parameter values from the examples of line trace are reasonably consistent, as are the two sets of surface parameters from the two samples of roughened steel. However, the values of height parameter are larger taken from the 3D surfaces because they sample the whole area which encompasses higher summits and deeper valleys than a single line trace. The skewness measured from the 3D surfaces is low and indicates that the distribution of height features across the surface is evenly distributed between summits and valleys. Skewness measured from a single line profile can vary much more because it does not sample so much of the surface.

The fractal dimension of the line profiles is close to unity and the fractal dimension for the surfaces is close to 2. This shows that the surfaces are not very complex. Studies have found that typical metal surface profiles have fractal dimensions of 2.3 or less [28] because impact by abrasive particles knocks sharp summits down and thus limits the ramification of the surface [29]. In a similar vein, the roughness ratio of these surfaces is only fractionally greater than one, so grit blasting the metal has not increased its surface area to several times its flat, smooth, value. These values are consistent with the view of the surface profile in the lower graphs in Fig. 2 and the impression given by the SEM images.

The gradient parameter is another way of measuring the tortuosity since the reciprocal of the cosine of the average angle is the hypotenuse divided by the adjacent side, which should also be the ratio of surface profile length to the scan length, on average. The average angle for these surfaces is approximately 33 degrees which is consistent with the other data. This seems reasonable since, statistically, no high-angle feature would survive continued bombardment.

No single parameter can characterize a surface profile and there is no consensus even on a group of parameters for that purpose. Interactions that determine adhesion or restrict the motion of water and electrolyte ions along the interface and the electrochemical processes of corrosion are all molecular processes that do not directly depend on the size and shape of features in the topological profile. Examining the various stages of coating, from application to curing and subsequent testing, elucidates which parameters that may be useful and significant.

3. Coating application

Coating thickness is usually decided by its use. If a coating must act as a barrier to water and corrosive salts, it must be thick enough to provide that protection for its design life. If a coating must survive mechanical impacts, e.g. when the infrastructure is buried, then it will be tougher if it is thick. Since metals are usually stronger and tougher than organic coatings it is beneficial for the mechanical integrity of the combination if metal peaks extend significantly into the thickness of the coating. A thick coating (~ 1000 μm) can be applied over a surface profile that has a height of several hundred micrometers. However, coatings that must also provide some aesthetic value cannot be applied over a high substrate profile because the substrate features would be difficult to obscure; they would cause texture and would limit the gloss of the coating. Economics may also limit the thickness of the coating that can be applied. The choice of coating thickness and substrate surface profile is usually the result of a compromise that may not be dictated by adhesion or corrosion protection.

Before the adhesion or corrosion protection of a coating can be considered, it must form a continuous film without any holidays or air voids. All application techniques share the problems of substrate wetting and thus defects. In general, spray droplet size or brush bristle size etc. have a large impact on how well paint enters the smallest features on a substrate. As an example, spray application is examined in more detail.

3.1. Spray droplet impact

Spray equipment is used to apply a variety of coatings in factories and in the field. The variation in equipment used is considerable, but one can expect the spray droplet size to be 20–200 μm with droplet velocities at the nozzle exit of up to 300 m/s [30,31]. Air entrainment within a coating or between coating and substrate is well known [32]. When a droplet approaches a surface rapidly the air below may not escape; it may be compressed and deform the droplet so that an air bubble is trapped underneath the liquid which remains if the paint cures or dries too fast for buoyancy to enable the air bubbles to escape [33,34]. Since many droplets arrive quickly there is the possibility that they may trap air underneath and in holes on the surface [35,36]. However, an uneven surface will allow air to escape from underneath a spray droplet if there is a channel leading away from the center of the impact. Wetting by a paint liquid also requires a low enough viscosity for a long enough period that the surface is covered, and air is excluded. Paint brush bristles and roller cover fibers have much the same size range as spray droplets. A surface profile thus must have features that

are wide enough for the liquid to penetrate its features within a suitable time. Rheology and wetting, and their rate of change during curing, also affect the ability of a coating to penetrate small features. Practical aspects of coating purpose and application often dictate the size of the surface roughness profile.

3.2. Wetting

If the liquid does not cover the surface completely, there are gaps or voids in which water and salt ions can accumulate and thus cause corrosion. Roughness can provide a barrier to spreading because the angle that a surface feature makes with the leading edge of the spreading liquid does not satisfy the balance of surface forces there, i.e. it cannot wet the surface there, and thus leaves a void.

The advance of a liquid over a flat surface is easily understood by Young's equation that links the contact angle, Θ, to the surface tension of the liquid etc [37]. This is written with γ conventionally representing the surface tension at the interface between two phases and using subscripts referring to the solid, liquid and vapor:

$$\cos(\Theta) = \frac{\gamma_{sv} - \gamma_{sl}}{\gamma_{lv}}$$

Obviously, it is better to have a liquid that spreads over the surface well by having a low contact angle.

3.3. Uneven surface

If the liquid is advancing over a surface with a change in slope upwards, then the liquid can advance because at the point where the slope increases, the contact angle becomes greater. The opposite is true when the advancing liquid front meets a change in slope downwards. As the liquid arrives at the change of slope, the geometry imposes a smaller contact angle, so it will not progress down the slope; it is "pinned". This is known as the Gibbs criterion [38,39]. The drop can only advance if more liquid arrives to make the drop protrude over the edge so that its equilibrium contact angle can be satisfied on the downward slope. On a rough surface, liquid may advance through a depression up to a summit on the profile but will be stuck there unless more material is deposited, and its leading contact angle can increase. After application ceases, its lateral extent may be defined by where it is pinned.

Dewetting [40], i.e. retraction of a liquid film into drops, or into a thicker film with gaps, on a substrate occurs if the layer is thin and if the liquid does not wet the material of the substrate very well. This is seen, for example for water on a newly waxed car, but is probably not a concern for a thick coating that was formulated for application to the substrates under consideration here.

For a coating to be competent, a spreading paint should remain in the "Wenzel" [41] state where the coating spreads into all the surface features and excludes air completely, i.e. it has a low enough contact angle (< 90 degrees) and none of the surface features cause the liquid to be pinned. In this case the apparent contact angle on the rough surface is related to the contact angle on a flat, smooth surface, Θ, by:

$$\cos(\Theta_{rough}) = r\cos\Theta \quad (1)$$

The roughness of the surface acts to diminish the measured value of the contact angle because the area over which it spreads is increased by the roughness factor, *r*. For example, if the roughness, *r*, is 1.2, and if the contact angle on a smooth surface would be 45 degrees, then the macroscopic contact angle on the rough surface is 32 degrees, according to Eqn. 1. Up to a point, roughness aids wetting. The relationship between the contact angle on a smooth surface and on a rough surface provides a value of *r*, and thus as pointed out above, the average slope of the surface.

If the contact angle is higher (> 90 degrees), Eqn. 1 means that the contact angle is made higher, i.e. poorer wetting. If the surface features are dense and have large changes in slope, it is possible that the liquid cannot get into all the depressions and valleys and thus rests on the peaks with voids underneath. This is the "Cassie-Baxter" state [41] and is part of causing surfaces to be self-cleaning (liquid drops imbibe dirt and roll off, leaving a clean surface). The transition to this state as peak density increases can be calculated for simple profile shapes [41]. Obviously, there is a chance that if the spray droplets are large enough and the surface profile peaks are sharp enough and close enough together that the liquid will span a valley and never fill in the void beneath. Coatings must have good wetting properties and there is an upper bound on surface peak density for any coating being used depending on its application properties.

Comparing liquid contact angle on a rough surface to that on a smooth substrate using Wenzel's equation provides a value of *r* and thus a value for the average slope of the surface. Measuring contact angle of a liquid precursor to the solid coating can be difficult due to solvent evaporation, changes in viscosity etc., and it requires specialized equipment, but it measures interfacial forces and characterizes the surface profile in ways that are important. Ultimately, however, the practical interest is in the interfacial forces of the solidified coating and how well the solid coating endures and protects the metal.

Important substrate characteristics for wetting are the surface roughness, *r*, and an upper bound on the density of peaks.

3.4. Substrate holes

These approaches to understanding how a paint could completely coat a rough surface profile implicitly assumed that the air trapped between the coating and the substrate could escape through a side channel. However, if there was a pit or hole in the surface profile, liquid can trap air and thus leave a void. De Bruyne [36] calculated this for a flowerpot-shaped hole or a shallow spherical depression.

The calculations use several parameters and demonstrate that understanding completely how a liquid wets a surface (which is crucial for adhesion) need more and different parameters that are usually recorded for a surface profile. A liquid coating may advance into the flower-pot shaped hole if $(\Theta + \phi)$ is less than 180°. Clearly if it is steep sided or "ink-pot" shaped (the bottom is wider than the top), ϕ is greater, and there is less likelihood of the liquid entering, depending on its contact angle. Equally clearly, liquids with a low value of Θ will succeed better in entering, depending on the angle of the side. If one simplifies the calculations by assuming a cylindrical hole and a contact angle of 90 degrees, the liquid will not enter at all, as should be expected. In practice, a coating might also solidify before it can reach its equilibrium wetting position within a hole, and a larger void than predicted will remain. Holes or fissures in the substrate seemingly might provide some mechanical anchoring of the coating and thus improve the measured adhesion, but if the coating traps air, then it becomes a place where water and electrolytes might concentrate and thus initiate corrosion.

4. Curing

4.1. Curing at an interface

The presence of a weak boundary layer at a polymer-substrate interface is often invoked in describing adhesion behaviour. If there is a specific interaction between one of the components of the coating precursor mixture and the substrate then, if the ingredient migrates fast enough there may be an enrichment or depletion at the interface [42]. This depends on the chemistry of the liquid coating mixture and the nature of the surface whether it be metal, oxide or conversion coating etc., but it cannot be assumed that the coating will be the same at the interface as it is in the bulk [43]. The very presence of the impenetrable substrate may mean that the crosslinking reactions are restricted because the reactants cannot approach each other from all directions and the degree of conversion near the substrate is less than in the bulk of the coating. In any case, the polymer chains at the impenetrable interface

cannot adopt all the conformations that are available in the bulk. Deposition or curing of a coating at an interface creates problems, regardless of the topology of the surface profile.

If water or other contamination is present on the substrate, it may affect the curing chemistry and damage the adhesion of the coating, e.g. water will form CO_2 gas with an isocyanate instead of reacting to form a polyurethane and blushing or blooming can affect an epoxy coating.

In addition to the (alkaline) hydrolysis of the coating polymer, normally proposed as part of the cathodic delamination process, if water is present under a coating, soluble metal ions may attack the polymer or create metal salts, from underneath [44,45]. The "Fenton" free-radical mechanism, usually involving iron [46], also causes oil paintings to deteriorate [47] but it also aids the break-down of plastic sheeting used in agriculture for mulching [48].

Thus, there are physical reasons as well as possible chemical reasons for the polymer near the substrate interface (an "interphase") to have poorer properties than in the bulk, i.e. a weak boundary layer. This layer will not only have disappointing adhesion but also it will be more open to water and electrolyte and be more prone to swell or shrink in wetting and drying cycles. Problems occurring near the substrate in the curing of a coatings may happen whether the surface profile of the substrate is rough or not. However, this region is important for both adhesion and preventing corrosion underneath a coating.

5. Solid coating films

Most metals have corrosion products that are less dense than the metal. As blisters or under-film corrosion grows, the coating becomes separated from the substrate by a peeling action at the periphery of the corroded region. It would be useful to measure coating adhesion using a peeling technique, but this is very difficult in typical circumstances.

5.1. Interfacial interaction

When investigating the variation of adhesion with coating composition an underlying assumption is that the measurement of adhesion will be sensitive to how composition changes the interfacial forces between coating and its substrate. However, there are severe difficulties, even with a smooth interface.

In order to measure adhesion of a cured coating to its substrate there is no option but to measure the energy or force that it takes to break them apart. Each of the mechanical geometries that might be used for this deform the polymer in their own way and produce their own pattern of stress concentrations [22,49], so the strengths measured depend on the method used to measure "adhesion" [50,51].

For coatings, there are three principal approaches to measuring adhesion. There is a class of qualitative methods that scratch or gouge the surface of a coating, with either a pencil of known "hardness" [52] or a sharp blade [53]. These tests are rapid and simple and can be done in the field as well as in the laboratory. The coating suffers a ploughing action that often relates well to how coatings must be durable in practice, and whether adhesion is intact, but these methods do not measure interfacial forces.

A second approach is to peel the coating away from the substrate. In principle, a peeling action requires comparatively little force to separate two materials and there is much less deformation of the adherends themselves, compared to the tensile pull-off test, so that the result is more characteristic of the interface. In practice, peeling is important because it is probably how the separation between the coating and the substrate takes place when corrosion occurs. In addition, if a failure is suspected in the field, a common approach is to lever (peel) a coating up from an edge, for example using a screwdriver. Controlled peeling of an existing, extensive coating is difficult because it must be done from an edge and coatings are difficult to grasp and are often too brittle to bend during the peeling. However, laboratory peel tests and variants, e.g. wedge test, four-point bending, double cantilever beam, blister test etc. are useful [54].

For polymer coatings, in many applications, the most common quantitative method is the tensile (or pull-off) test [17]. This uses a metal stud that is glued to the coating and then pulled off hoping that the failure will occur at the coating-substrate interface and that the stress represents the strength of the interface. This is a test that can be performed on any existing coating but has many problems [55,56]. Problems include the fact that the stress is not even across the test area since there is a stress concentration around the rim of the stud and coating; if the metal stud is not perfectly perpendicular to the coating the misalignment tends to provoke a peeling behavior and thus gives an artificially low value; the common practice of scoring the coating around the rim of the coating to define the area tested can easily damage the joint before the test. However, the test does generate a number for the overall strength of the coating-substrate joint.

A typical result for the pull-off test might be a stress, σ, of 13.78 MPa (2000 psi) using a coating thickness, $t_{Coating}$, of 762 μm (30 mil) [56]. If the bulk modulus, K, is 6.67 GPa (Young's modulus of 2 GPa with Poisson's ratio of 0.45), using Kendall's equation for pull-off strength [57],

$$\sigma = \sqrt{\frac{2KG}{t_{Coating}}}$$

estimates that the fracture energy, G, to be 10.8 N/m (J/m^2). This value is typical of many other results for similar experiments. Kendall's equation holds for an interface without a significant defect where the coating is thin compared to its lateral extent [49].

Another approach to estimating interfacial forces and adhesion is via the surface energy and contact angle of liquid analogues to the cured coating. The work of adhesion, W_{sl}, between substrate and a liquid coating is given by the Young - Dupré equation [37],

$$W_{sl} = \gamma_l(1 + \cos\Theta)$$

Where γ_l is the surface tension of the liquid which has an equilibrium contact angle of Θ on the (flat and smooth) substrate. The highest surface tension, approximately 50 mN/m (mJ/m^2), is found for epoxies and similarly polar organic liquids. Thus the "thermodynamic" work of adhesion, W_{sl}, is 0.1 N/m (J/m^2) at most, if the contact angle is zero.

This calculation assumes that interfacial, intermolecular forces do not change when coating solidifies. Clearly this is seldom true because solvent evaporates, coating chemistry changes during cure and there may be additional bonds formed with the substrate during cure. Unfortunately, this estimate is used in the literature often without any warning of its limitations.

If the van der Waals and polar bonding at the interface does not change significantly when the coating solidifies and no ionic or covalent bonds with the substrate form during cure, this is an approximation for the interfacial energy of the solid coating. This value is 100 times less than the estimate from the pull-off test. The discrepancy between the "thermodynamic" work of adhesion and the "practical" or "apparent" work of adhesion has been recognized and identified for several decades [22,58]. Some of the difference is because the thermodynamic work of adhesion assumes that there is no contribution from parts of the polymer chains that are connected to the moieties at the interface. It is difficult to see how any effort expended in separating the two materials avoids the need to deform connected and neighbouring parts of the polymer molecules, so the minimum work associated with propagating the separation crack must be larger than the thermodynamic work of adhesion deduced from liquid equivalents. The major contribution to the difference is that the overall energy expenditure, or force at failure, is dominated by the deformation and viscoelasticity in the bulk of the coating, especially when the detachment is rapid, as in the typical pull-off test [57,59,60].

If the rough surface causes the failure of the joint to be within the coating, then the tensile adhesion stress is determined by the strength of

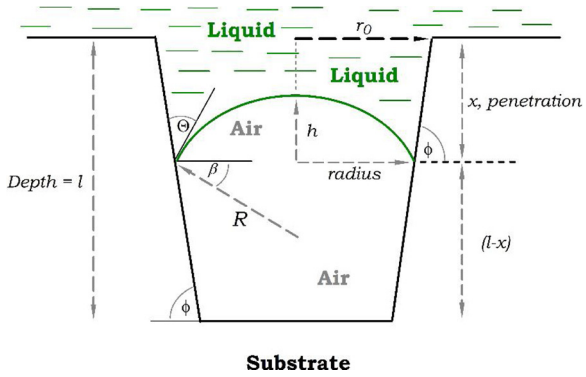

Fig. 3. Parameters used in De Bruyne's calculation of the penetration of liquid that completely covers a flower-pot shaped hole.

the coating and cannot quantify the effect of the surface roughness. However, one might expect to see some correlation between surface roughness and tensile adhesion if the same coating was used on a variety of surfaces, and all the fractures were completely interfacial.

In addition, the standard deviation in tensile adhesion results is often 10 % of the mean value [56], i.e. 10 times larger than the thermodynamic work of adhesion. Such variation would completely obscure any trend in the data caused by systematic variation in the compositions that altered the thermodynamic work of adhesion. Pull-off adhesion tests are unsuited to investigate the interaction of materials at the interface.

Peeling adhesion test geometry can give results that approach the thermodynamic work of adhesion but, to achieve this, must be done at extremely slow speeds [58,60,61].

Quantitative investigations of corrosion protective coatings' adhesion are often done in conjunction with the effect of surface roughness (Fig. 3)

5.2. Failure mode at a rough interface

At the interface, the stress which affects the molecular interfacial bonds depends on the local slope and can be resolved, in 2D, into two components, Fig. 4. One component is perpendicular to the interface, and the second is along the interface.

No matter how steep the interface is, the external force operates

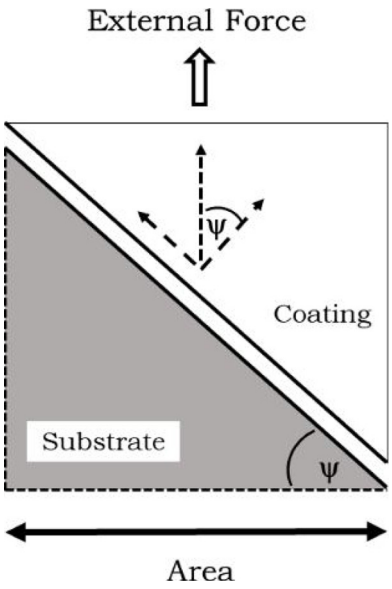

Fig. 4. 2D representation of the external load resolved into components on an oblique facet of the interface between two materials.

over the same projected (normal, flat) area, so the increased surface area gained by surface roughness does not reduce the stress because the load is distributed over a greater area, although this is often proposed in conversation. The roughened interface helps, but in a less direct way. In Fig. 4, the component perpendicular to the interface acts in a tensile, opening mode. The component parallel to the interface pushes (or pulls) one material along the other, shearing the interface.

When considering the way in which fractures progress, loading is characterized by three modes [49,62] Fig. 5. The tensile, opening mode is labelled Mode I. In this, the crack front is a line perpendicular to the stress. Mode II loading or fracture is a sliding shear over an area in the plane of the crack. Mode III is also a shear mode but with a tearing action across the contact area, sometimes called a "trousers" mode. Mode III does not arise in Fig. 4 but can be imagined on a rough 3D interface. Mode II and III are terms not often used in coatings' literature, instead this shear possibility at the interface is often described as providing "interlocking" or contributing to interfacial friction via an effective coefficient of friction [63].

In an homogeneous brittle solid, cracks proceed approximately along a path where they open by Mode I only, i.e. where there is no Mode II resistance [49,64,65]. If they encounter some Mode II resistance, the direction changes to minimize this. Crack progression between two different materials is much more complicated because the two materials and the interface have their own, different values of toughness and failure stress, for each of the possible modes. Pure Mode I loading is weak because, crudely, only the bonds on a line across the fracture oppose the failure. Mode II, and III, provide greater resistance because the bonds over an area of the interface are resisting the load. One could see how a surface with many deep, vertical pits would provide high adhesion from a great deal of Mode II anchoring. However, those pits would be very difficult to fill with liquid coating.

From these considerations, the average slope of a surface should be a useful parameter to measure and record because a higher value signals a greater chance of Mode II etc. loading which would increase the strength. In addition, the slope may act to diminish the stress in the Mode I direction below the Mode I failure stress of the material. The variation in slope, perhaps through its standard deviation, would also be useful, because a widely varying slope would show that the surface has a significant fraction of places where there was little advantageous Mode II loading and *vice versa*. In addition, the average angle also can be used to calculate the developed surface area, *r*, from the reciprocal of its cosine which gives the ratio of the hypotenuse to the adjacent length. This ratio, for a line profile, when squared should give an estimate of the developed surface area.

When the term "interlocking" is used to describe a roughened surface, it should imply the possibility of Mode II in addition to Mode I rather than assume that it has connotations of dovetailing or overhanging features, which were rare on the abrasive blasted surface examined here. This mixture of loading modes is sometimes called "mixity". An example of how interlocking might be better visualized is to think of finger (comb) joints often found in wooden products. A dovetail joint uses a flared mortice and tenon.

5.3. Tensile adhesion testing and roughness

For illustrative purposes, adhesive fracture can be described simply by linear elastic fracture mechanics using the Griffith equation [66]:

$$Stress_{\text{Failure}} = \sqrt{\frac{2E(G - U_{Internal})}{\pi c}} \quad (2)$$

Where:

E = Young's modulus

G = a measure of toughness

= energy required to create new crack surface area at the interface (strain energy release rate)

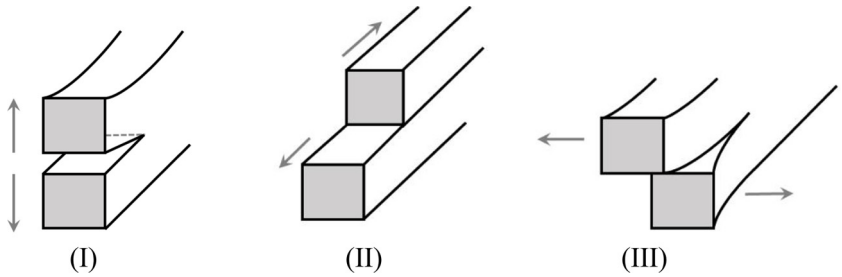

Fig. 5. Fracture modes. Mode I: tensile opening; Mode II: in-plane shear; Mode II: out of plane shear. The arrows indicate the relative movement of the components.

c = radius of the largest existing crack or defect (assuming a circular shape)

Eq. 2 includes the effect of internal strain energy, $U_{Internal}$, which would arise from curing shrinkage or swelling etc. and diminish the effect of G, and thus the stress required for failure. Griffith's equation can be used when there is already a crack and the boundaries of the material are distant so that it is the stress concentration around the crack tip that governs behavior [49].

Tensile adhesion testing pulls the coating away from any sharp peaks in the metal surface. If the coating were compressed onto these features, then they would produce stress concentrations in the coating.

There is a large mismatch of modulus across the interface when a polymer coating is on a metal substrate and the stress field at the crack tip, dictating its likely direction, is a function of this mismatch via the Dundur's parameters [49,67]. At the tip of a crack, the stress is inhomogenous and the stress vector very close to the tip changes direction with distance [49,68] so an interfacial (adhesive) failure may kink into a weak adherend, becoming a cohesive failure, depending on how the toughness of the material compares to the toughness of the interface. If the crack is diverted into the coating and the coating can absorb some of the mechanical energy through plastic deformation (due to composition, temperature or testing rate) then the propagation of the crack may stop. In this case the crack is "blunted" making the joint stronger. If the interface is rough, i.e. changes direction frequently, then there is a greater chance of this blunting behavior as well as the advantages of Mode II loading and a reduction in the Mode I stress. If an adhesion test is used to gauge the integrity of a polymer coating on a metal substrate, then it is always taken as a good sign if the test produces a cohesive failure within the coating.

Roughness increases the surface area, but calculation of external stress is not affected because its component in the tensile, pulling off, direction does not change when the local slope is not perpendicular to the stress. However, the increase in area developed by the roughness results in more bonds (of any type) between the two materials over a unit (projected) area [60]. The interfacial energy, G, becomes larger, i.e. rG, making the fracture stress increase by a factor of $\sqrt{r}$. Using the values of r in the tables above shows that G might increase by 25 % and thus increase the fracture stress by 12 %, which is not a very substantial effect. Developed surface area values found elsewhere for a variety of surface treatment techniques [69] are similarly all fractional with the largest, 49 % (equivalent to an increase in fracture stress of 22 %), resulting from grit blasting. As stated above, if the tensile pull-off adhesion method is insensitive to the interfacial forces, then this effect of surface roughness may not be apparent in this form of conventional testing. Roughness probably has a greater effect in how the local slope affects the mixture of loading, or failure, modes.

Fig. 4 shows that the loading will have a greater component of Mode II at steeper angles, increasing with sin (ψ). Rough interfaces engage this mode more than smooth interfaces so the energy (or force) necessary to cause interfacial joint failure will be enhanced, and thus increase the measured value of adhesion. A quantitative comparison of Mode I and Mode II toughness, G, has for an epoxy on an aluminium alloy, $G_{Mode\ I} = 1.0\,\mathrm{kJ\ m^{-2}}$ and $G_{Mode\ II} = 5.4\,\mathrm{kJ\ m^{-2}}$ [70], so it is indeed more difficult to have a failure in Mode II loading. It is accepted that mechanical energy required to cause a crack to propagate is not only much larger than the thermodynamic work of adhesion, but also it increases as the fraction of Mode II loading increases [65].

At an angle, the component of the force in the Mode I direction, perpendicular to the interface, will be diminished according to cosine (ψ) in Fig. 4. Depending on the material, there may be an angle above which that stress component is reduced enough to avoid interfacial failure by tensile opening, thus strengthening the mechanical adhesion. Using a value of 33 degrees, representative of the example surface presented earlier, the force in the Mode I direction would be 84 % of the pull-off force and the component along the interface would be 55 % of the overall value. It is tempting to say that we could calculate the average profile angle that would be necessary to protect a particular coating-metal combination in this way but measuring the necessary mechanical and adhesive properties of any polymer-substrate combination would probably be too laborious.

5.4. Peeling and surface roughness

An adhesion failure via peeling does not need the high forces that the tensile test does because there is only a line of disbondment rather than an area and the deformation of the coating, in principle, remains constant as the peeling progresses. In general, one measures the force, F, necessary to peel the coating of width, w, from the substrate. If the coating is peeled perpendicularly to the substrate, then,

$$\frac{F}{w} = G - U_{Internal}$$

This equation is derived from a simple energy balance [71,72]. G, again, is the energy required to overcome adhesion (although its value will be very different from that in the pull-off test) and $U_{Internal}$ is included again to show how the effect of curing shrinkage strain energy would diminish the adhesive strength. In fact, the mechanics of peel testing are complex and, as for the pull-off test, the results are dominated by the mechanical properties of the polymer [73]. However, in this case peel strength depends linearly on G (and thus rG), so the increase in surface area developed by roughening, and the concomitant increase in the number of interfacial bonds, should have a greater effect than it does on pull-off measurements, and thus be more important and observable.

Peeling experiments are done in several variants, e. g. double cantilever beam, wedge test, four-point bending, blister test etc. and focuses on steady-state propagation of a crack rather than on its initiation and it can be done at very low rates. Experiments done over a range of speeds demonstrate that at very slow rates, the energy required to overcome adhesion gets much closer to the thermodynamic work of adhesion [58,60,61] than does the pull-off test, but as pointed out earlier, any adhesion test involves more work than just against the interfacial forces between neighbouring molecules.

Peel failure load, F, has been shown to increase with surface roughness [74,75] but, like all experiments examining failure, peel test results show a considerable experimental fluctuation and it can be

difficult to separate the effect of roughness from changes in surface chemistry, depending on how the metal surface was treated. There are several studies of adhesion on surfaces with carefully controlled or patterned roughness [76] that show an increase in interface toughness when grooves are closer together and when they are deeper, attributed to deformation of the adherends and their cohesive failure [77]. These experimental studies all show that interfaces are stronger when the roughness features are steeper. There are many theoretical mechanical analyses which show how idealized surface profile features (steps, triangles etc.) increase the stress or energy necessary to cause a failure to propagate via mixed mode loading and diversion of the crack into the polymer where crack blunting can act [65,68,78–80]. These all show that the reinforcing effect is greater as the overall steepness of the interface increases.

In general, descriptions of the effect of loading modes deal with geometry, not the absolute size of the features. If the size of the yield zone for the polymer [49,78] is larger than the features at the interface, then the effect of each loading mode is averaged in some way with the effect of the others, but the benefit of engaging Mode II would still be present. This should also occur on a surface that has nanoscale features because the stress on even one molecular bond depends how it shares the load with others and the direction of the load.

It is in the peeling mode of adhesion that the effects of peak height and peak spacing might be best identified on roughened interfaces. Details, not accessible through experiment or idealized analysis, can be found in computational stress analysis of roughened interfaces. Finite element analyses of peeling at interfaces with sinusoidal profiles have shown that increasing the peak-to-valley height slows crack growth in elastic materials [81,82]. The analyses show that there are stress concentrations near the sharper turns in the profile, but the overall result is that joint strength is improved as the ratio of the amplitude to the spacing of the peaks increases, i.e. by steeper profiles. When plasticity is allowed in the material properties, crack blunting [78,83] is seen when highly localised deformation occurs in the polymer at the crack tip. Effectively the joint is toughened. When the surface profile has small peaks distributed on the larger peaks, it is the larger features that seem to dominate the toughening of the interface through crack blunting [84].

A roughened surface enables a greater number of bonds between the materials, Mode II loading and there is more chance for the stress energy or crack to be limited by the polymer. These aspects are functions of shape variations along the interface and do not depend on the absolute height, or depth, of the profile. The absolute height of the profile and the absolute coating thickness are decided by other issues. It is difficult to find an experimental study of the effect of roughness on adhesion that quantifies the effect of the coating thickness since the focus is usually on the interface. Computational studies focus on the profile at the interface with material boundaries that are far away and do not influence the stress fields. It is clear, nevertheless, that a substantial profile height tends to give a higher apparent adhesion value than less. Wetting sets limits on the ramification of the substrate. Remote from the interface, increasing the penetration of the metal into the polymer coating by having higher peaks strengthens the joint and the coating against external forces, including adhesion testing. The thickness of the coating (and thus the profile height) is determined by the requirements of being a corrosion barrier. As mentioned above, a practical example of a high profile and Mode II loading is the finger joint approach to joining shorter lengths of wood. Other examples are ground anchors and rock bolts which rely upon perpendicular holes which are deep compared to their diameter in order to achieve the anchor strength [85,86].

5.5. Soft coatings

Some protective coatings are comparatively soft. A contribution to the resistance at an interface that is not a function of the interfacial forces, is cavitation, which plays a considerable role in the performance of soft pressure sensitive adhesives [87]. Above a critical stress, cavities form in the soft adhesive in an analogous way to cavitation in liquids, e.g. around ships' propeller surfaces. A rough surface might also already have entrained voids and air pockets which may expand in the cavitation process. Within the variation of crosslinking density in pressure sensitive adhesives the cavity is a pancake shape for those having higher cross-linking density (stiffer) [88]. Such cavities spread quickly, since the stress is concentrated around their periphery, and coalesce as external load increases, bringing failure at a small strain within the polymer layer. Presumably changes in slope on the surface profile might slow the enlargement of these pancake-shaped cavities in the same manner as above when the change in slope brings Mode II into play rather than a simple Mode I. This phenomenon occurs in softer pressure sensitive adhesives, with molecular weight between crosslinks $> 10^4$ [89]. Materials with higher crosslink density seem not to engage this mechanism so this will not be a factor for the harder coatings, e.g. epoxies or polyurethanes, used as protective coatings. In soft coatings, cavitation will contribute to the value of adhesion measured but have very little to do with the interfacial bonding that might affect the diffusion of water and ions along the interface.

There is no single characteristic of a surface profile that determines its influence on adhesion. At the interface, an increased surface area increases the number of bonds and steep angles at the interface engage Mode II loading. If the average angle and the developed surface area are not explicitly available from profilometry, two commonly measured quantities, *Ra* and peak density (peaks/length) can be easily combined to calculate an approximation for them.

5.6. Water and the interface

Corrosion creep from a gap in the coating always seems to be more rapid than corrosion starting under the coating barrier. One study that quantified the two paths found that the diffusion coefficient of water through a coating [3] was 6×10^{-13} m^2/s, but the diffusion coefficient of a sodium ion along the interface between the same coating and a (smooth) metal substrate was 100 times faster, 6.4×10^{-11} m^2/s [4]. That work determined that transport of ions controlled delamination kinetics but the action of ions requires the transport of water, as well.

5.7. Molecular scale

If they do not self-passivate, rough metal surfaces can corrode faster than smooth metal surfaces [90] because they have a larger surface area accessible to the environment and atoms at steps on a metal surface can be attacked more easily but the presence of a coating changes the local electrochemistry and access to the surface. The advance of water molecules between polymer and metal will be governed by a process that depends on the compatibility of the water with the materials on either side and the entropy increase permitted by the mobility of the polymer in the coating (if we assume that the metal side is impenetrable). A water molecule could not move into a location unless the polymer segment there had moved away.

An approximate way to look at compatibility in this situation is to consider the Bjerrum length, λ_B, of a material [91]. This is the distance over which the electrostatic interaction between two charged species diminishes to become comparable to thermal energy k_BT (k_B = Boltzmann constant and T temperature in Kelvin). If the charges are closer than λ_B then electrostatic forces control charge movement; if further apart, then random thermal motion dominates. For singly charged ions,

$$\lambda_B = \frac{e^2}{4\pi\varepsilon\varepsilon_0 k_B T}$$

e = electronic charge
ε_0 = permittivity of vacuum
ε = relative permittivity of the material

The relative permittivity of a crosslinked coating polymer might be $\varepsilon = 5$, approximately. In this case, the Bjerrum length is 11 nm at normal ambient temperatures (300 K), but the distance between polar groups on a typical epoxy or urethane polymer binder will be much closer, helping the hopping of a charged molecule or ion to a neighbouring polar group on the polymer at the interface. Partial charges on a polar group in a polymer and on the water molecules in the gap will be a fraction of the electronic charge, so the Bjerrum length will be reduced from 11 nm, but polar groups on an epoxy or urethane are probably still dense enough to permit charge hopping. If the material on the other side of the interface is a metal, or an oxide or hydroxide, then polar groups on that side will be very close together compared to the density on the polymer side so the migration of water along the interface is probably strongly encouraged by the metallic side as well. The compatibility of the interface provides an enthalpic contribution to how the water can spread there. The very species that are employed to enhance the adhesion of a polymer, polar groups etc., may have a deleterious effect in the longer term because they are compatible with water [43]. The connection between adhesion and corrosion protection is not simple especially since the two phenomena are usually measured at different times and under different circumstances.

It is well known that crosslinked polymers contain many defects [92] but, as pointed out earlier, the polymer at the interface probably did not form even as well as the polymer in the bulk, so the interface will provide molecular scale defects that provide more opportunity for the faster diffusion of water etc. [93] and, in the absence of strong interfacial interactions, polymer segments there may be more mobile thus allowing the entropy of the water molecules to increase through their diffusion across the interface. This weak boundary layer and the polarity of the materials on either side of the interface provide ready (entropic and enthalpic) explanations for why water and salt diffuse across the interface so much faster than they can diffuse through the bulk of a barrier coating.

In principle, both an immobile polymer (higher glass transition temperature) [43] and nonpolar materials at the interface will slow the diffusion of water and other species along the interface. Modern, low VOC, strong, highly adhesive polymer coatings, which are easy to apply, use crosslinking chemistry which implies polar or hydrogen bonding materials. This might be counterproductive in the sense of compatibility for the long term diffusion of water and ions along the interface but, on the other hand, sufficient crosslinking should also reduce the polymer and electrolyte mobility at the interface.

5.8. Macroscopic scale

A simple, but instructive, thermodynamic description for the stability of an adhesive bond in the presence of a liquid was developed some time ago [94]. If water wets both adherends then the dry adhesion forces between them are replaced by interactions of each surface with water and only the water provides a force holding the joint together. Adhesion between a metal (hydr)oxide surface and a typical, somewhat polar, organic polymer coating is almost certain to be completely disrupted eventually by water. Adhesion at an interface between hydrophobic materials would be stable [95] because water would not intrude between them. Many commercial metal surface treatments decrease the hydrophilicity of the metal surface as well as passivating it and making it rough, both of which improve the environmental durability of the coating – metal interface.

The Griffith equation, Eqn. 2, also shows several other reasons why adhesive strength is reduced if liquid water is present. Modulus, E, will be reduced via plasticization. If water wets the adherends then, as discussed previously, the interfacial energy, G, is much reduced. Any flaw from which fracture propagates, c, may be larger when water is present, e.g. an incipient blister. Swelling stress induced in the polymer by the water, will mean that less external stress is necessary to overcome the adhesion. Pull-off adhesion is very sensitive to the presence of water and a low value in the field in wet conditions is an indicator of water intrusion. After drying, restoration of good adhesion is encouraging but it is probably true to say that any signs of water affecting adhesion indicates a strong possibility of corrosion in that joint in the future, since the metal and the polymer probably suffered permanent changes.

6. Roughness and corrosion

6.1. The advance of corrosion

The rate of corrosion creep under a coating is difficult to follow but various techniques have been applied, e.g. infrared spectroscopy [96]. Scanning Kelvin probe microscopy does not detect water or electrolyte ingress directly but has been used to track the delamination front under a coating via the change in work function caused by water and ions [4,63,97,98].

Quantification of substrate roughness is sometimes also presented when the spread of corrosion is studied [99,100]. Other studies link corrosion spread with surface profile although it is sometimes difficult to separate the effect of variations in physical profile from simultaneous variation in surface cleanliness or surface treatment [8,10,12,69,101]. One study evaluated adhesion by peel strength and demonstrated a correlation with rate of electrolyte ingress [98] using scanning Kelvin probe microscopy. Where trends are measured, regardless of the instrumental technique or the materials or the interface roughness, the spread of corrosion or its surrogate, e.g. delamination, usually follows the square root of time, $t^{1/2}$ [2,63,69,96–99,102].

Dependence on the square root of time is the characteristic of simple diffusion behavior:

$$\langle x^2 \rangle = 2nDt \tag{3}$$

Where:
x = displacement
n = dimensionality
D = diffusion coefficient

Penetration of liquid into a capillary, which is like penetration between a substrate and a coating, also has $t^{1/2}$ dependence according to the Washburn equation. However, rates of delamination [99] do not match calculations using the Washburn equation if one uses values of surface tension and viscosity etc. typical of bulk water. In fact, there is no guarantee that corrosion in a confined space will be initiated through commonly accepted electrochemistry [103] and one must also be aware that the structure of water confined in 2 dimensions at an interface is still the topic of research and may not have the values of physical parameters that are typical of bulk water [104,105].

The spread of water, ions and, presumably, corrosion depends on the overall path length for their diffusion at the interface [9,63,99]. If the time for corrosion, or delamination, to reach a location depends on the square of the distance travelled, eqn. 3, then surface roughness has an effect equal to the square of the increase in length of the interface profile, i.e. tortuosity squared. On an isotropic surface, this would be equal to the developed surface area ratio, r. Values of r, for the surfaces in Fig. 1 and 2 and tables 1 and 2, were ~1.25 %, so, in these examples, the spread of corrosion would be slowed only 25 % over the rough profile. The developed surface area ratio may affect the rate of corrosion creep and the apparent adhesion strength, but through different mechanisms.

Another possibility, for how surface roughness affects corrosion creep, stems from combining ideas proposed for the process of cathodic delamination [2,106] and the loading mode ideas discussed earlier. In cathodic delamination, loss of adhesion opens a crack somewhat ahead of the extent of corrosion wherein water and salt advance. The coating is peeled from the metal by several mechanisms where corrosion occurs. Corrosion products are almost always less dense than the metal, so corrosion pushes the coating away from the metal; polymer at the

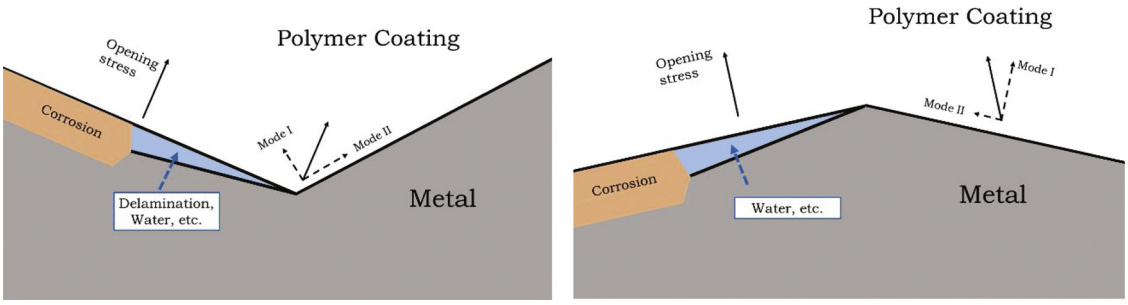

Fig. 6. Coating delamination by corrosion processes changes from mode I opening to a mixed mode where the direction of the surface profile changes.

electrochemical cathode on the metal is often hydrolyzed and thus loses adhesion. In addition, any swelling of the polymer coating by the water produces a stress that also aids delamination and may even buckle the overlying coating film.

The advance of delamination should be controlled by changes in the slope at the interface and whether the delamination stresses are acting in Mode I or Mode II, as in the prior discussion. If the angle of the interface changes from where the corrosion is currently forcing the two materials apart, the crack ahead of the corrosion must be restricted by the need to overcome the Mode II component where the gradient changes, as in Fig. 6. Presumably, this slows the lateral progress of corrosion over the metal surface.

In addition, if this delamination crack enters the polymer, the water and salt would be diverted away from direct contact with the metal. Entering the polymer may also "blunt" the delamination, as discussed earlier, so delamination might be halted. A rough surface profile, via fracture mode mixity, may slow the spread of corrosion.

If the topography of the abrasive-blasted surface were isotropic and random, the spread of corrosion would still proceed with approximately random-walk kinetics, i.e. $(\text{time})^{1/2}$ because the slope changes would be at random places, in random directions [107].

In common with the connection between adhesion and surface roughness profile, the two profile parameters that seem most likely to connect the rate of corrosion creep with roughness are the increased path length (squared), given by r, and the average slope of the profile (and its variation) where surface direction changes introduce Mode II loading which hinders cathodic delamination.

Conventional measurements of adhesion are essential to establish the quality of the coating application and curing process and are very sensitive to the presence of water. Current methods of measuring adhesion of cured coatings may well be affected by the interfacial profile but results are determined at a distance from that interface and the influence of that interface is obscured by mechanisms within all the materials between the measurement device and the interface. Corrosion involves reactions at the interface and the spread of corrosive species is controlled by the properties of the solid coating molecules at, or near, that interface and the interface topology. The spread of corrosion and coating adhesion may both be affected by same characteristics of the surface profile, but there is no exclusive and simple link.

7. Summary

Despite the plausible idea that the adhesion of a coating must be linked to its ability to restrict the rate of corrosion on a metal substrate, it is very difficult to find a quantifiable link. One basic problem is that adhesive interactions and corrosion occur at the interface on a molecular scale, but solids' adhesion is measured macroscopically and remotely from the interface. Results from typical adhesion measurements, even peeling, are dominated by the mechanical properties of the coating and are thus insensitive to the interfacial forces between coating and metal.

Peel testing is usually very difficult to perform for a coherent, solid coating that adheres well to the substrate. However, the pull-off test is comparatively easy to do and is a good indicator of overall coating integrity and whether water has intruded. A macroscopic measurement of adhesion may give a value that seems good, but corrosion may still be present in small regions, so good adhesion values are not completely reliable predictors of long-term protection.

Increased surface area developed by a roughening process means that there can be more interfacial bonds over a given span but pull-off stress depends only on the square root of that relative increase. The effect of that relative increase will be seen more readily in peeling adhesion because the peel force increases linearly with the interfacial energy. However, a roughened surface also increases adhesion because the external force must overcome Mode II shear loading on the inclined planes of the profile where also the Mode I stress component is diminished. Ever steeper inclinations on the surface would help the mechanical adhesive strength, but there is a practical limit to what abrasive techniques can achieve and it is difficult for liquid paint to penetrate completely into steep valleys. The terms "interlocking" or "anchor pattern" might imply dovetailing features on a surface and so can be slightly misleading where the term "interdigitation" is probably more descriptive. Although the focus here is on coating-substrate adhesion, similar factors must connect particle topography to pigment-polymer adhesion. Overall coating strength and toughness, as reinforced by the substrate, increases when the metal intrudes into the coating; how much this can be permitted is related to the thickness of the coating required for barrier properties. Compromise is necessary in choosing an optimum, practical surface profile.

An interface that changes slope also provides opportunity for fracture to be diverted into the coating, away from the materials' interface. There the dissipative properties of the coating absorb mechanical energy and may reduce it below the level necessary for fracture. If a roughened surface profile causes the failure to be within the coating, not at the interface, the connection between the characteristics of that surface profile and the result of an adhesion test must be diminished.

The increased surface area of a roughened interface slows the diffusion of water and corrosive ions according to the square of the relative increase in path length. On a randomly roughened surface the relative developed surface area should correspond to this. However, this slowing of corrosion creep might not be a usefully large effect because the relative increase in surface area developed by typical abrasive-blasting is only a fractional change, not a multiple. Changes in slope on a rough surface may be effective in slowing cathodic delamination by an additional mechanism. In standard descriptions of cathodic delamination, a crack ahead of the rusted region is envisioned within which water and electrolyte spread. This crack might be slowed when the delamination opening stress, which would be largely Mode I, is forced by a change in direction of the surface to overcome Mode II resistance as well. The delamination may also be slowed (blunted) if it is diverted into the polymer coating, which will also remove the corrosive species from direct contact with the metal. If these ideas are correct, both corrosion creep and apparent adhesive strength are improved by the increased surface area and changes in slope on a rough

surface. However, any correlation between corrosion protection and adhesion data is unlikely to be simple.

Developed surface area and profile gradient are linked and depend on the shape of the profile, not on the absolute size of the height variation. These parameters should be measured in addition to the height and peak density characteristics more often measured as quality control of surface abrasion. In fact, if peak height is multiplied by peak density the resultant quantity could be a useful comparative expression of the slope of the surface and thus the increased surface area. The average angle of a surface and the developed surface area can both be calculated more directly from the data recorded by a stylus profilometer. They could also be determined by careful measurements of the contact angle of a liquid coating analogue on the rough profile and on a smooth surface of the same material.

There do not appear to be simple criteria for choosing the best polymer coating. Inevitable imperfections deriving from film formation at an interface and the polarity of typical polymer coatings and metallic surfaces mean that water and electrolyte will diffuse across the interface faster than they can diffuse through a polymeric, barrier, coating. One approach would be to try and make the coating and the metal surface as hydrophobic as possible. On the other hand, the polarity of a coating, a result of crosslinking chemistry, improves adhesion, rigidity and other properties. One can appreciate the interest in surface profile as a separate route to improve adhesion and corrosion protection independent of composition. There is another compromise, between a glass transition temperature that denotes some toughness and crack blunting ability, i.e. $T_g \sim T_{service}$, and avoiding mobile polymer segments at the substrate that would allow water and salt to diffuse easily, i.e. $T_g > T_{service}$. Increasing interfacial adhesion strength is not the only way to impede diffusion of water and electrolyte along the interface, another approach is to increase the intrinsic rigidity of the polymer segments at the interface. Other, obvious factors that influence coating composition are that the polymer must resist environmental attacks, e.g. photodegradation. Any paint formulation must be mobile and easily wet the surface of the metal. Polymer coatings, like all material technologies, necessitate compromise.

There is no simple connection between adhesion test results, corrosion creep and surface profile. Protection of a metal using an organic coating is not only linked to adhesion but also other properties of the coating and the metal. Achieving improved corrosion protection requires greater understanding of how the bonds between coating and substrate impede the passage of water and electrolyte along the interface. There is no experimental technique available at present that can examine that interface directly so computer simulations are probably the most promising possibilities for better understanding, at present.

This review has tried to elucidate how a rough surface increases the apparent adhesion measured at any time and slows corrosion creep, but that does not guarantee survival in long term exposure to an aggressive environment. Significant, additional longevity can be achieved by changing the chemistry of the metal and the polymer at the interface for which there are many possibilities, both commercial and in research.

Declaration of Competing Interest

The author declares that there are no known competing financial interests or personal relationships that could have appeared to influence the work reported in this paper.

Acknowledgements

This review was provoked by colleagues and associates, principally Dr. Allen Skaja of the Bureau of Reclamation and Brent Keil of Northwest Pipe Inc., who asked seemingly simple questions which I could not answer to my own satisfaction.

References

[1] S.G. Croll, Electrolyte transport in polymer barrier coatings: perspectives from other disciplines, Prog. Org. Coat. 124 (2018) 41–48.
[2] P.A. Sørensen, K. Dam-Johansen, C.E. Weinell, S. Kiil, Cathodic delamination: quantification of ionic transport rates along coating–steel interfaces, Prog. Org. Coat. 67 (2010) 107–115.
[3] A. Leng, H. Streckel, M. Stratmann, Calibration of the Kelvin probe and basic delamination mechanism, Cor. Sci. 41 (1999) 547–578.
[4] A. Leng, H. Streckel, M. Stratmann, The delamination of polymeric coatings from steel [Part 2]: first stage of delamination, effect of type and concentration of cations on delamination, chemical analysis of the interface, Corr. Sci. 41 (1999) 579–597.
[5] Definition - What Does Adhesion Mean? (2020) (accessed 12th April, 2020), https://www.corrosionpedia.com/definition/5414/adhesion.
[6] D. Tordonato, Adhesion testing: how much is sufficient? JPCL 35 (11) (2018) 11–16.
[7] R.A. Dickie, Paint adhesion, corrosion protection, and interfacial chemistry, Prog. Org. Coat. 25 (1994) 3–22.
[8] J. Gooden, Myth or Fact: Higher Surface Profile Increases Coating Adhesion (Part 2), July 24, 2017 https://www.corrosionpedia.com/2/4862/procedures/myth-or-fact-higher-surface-profile-increases-coating-adhesion-part-2 (accessed 12th April, 2020) (2020).
[9] D. Greenfield, D. Scantlebury, The protective action of organic coatings on steel: a review, J. Corros. Sci. Eng 3 (5) (2000) 1–13.
[10] H.J. Roper, R.E.F. Weaver, J.H. Brandon, The effect of peak count on surface roughness on coating performance, JPCL 22 (6) (2005) 52–64.
[11] A.W. Momber, S. Koller, H.J. Dittmers, Effects of surface preparation methods on adhesion of organic coatings to steel substrates, JPCL 21 (11) (2004) 44–50.
[12] S.S. Jamali, D.J. Mills, Steel surface preparation prior to painting and its impact on protective performance of organic coating, Prog. Org. Coat. 77 (2014) 2091–2099.
[13] A.S. Bulick, C.R. LeFever, G.R. Frazee, K. Jin, M.L. Mellott, metal adhesion and corrosion resistance properties in waterborne, styrenated acrylic direct to metal (DTM) resins, Proceedings European Coatings Show Conf. Nürnburg, Germany, 2017 April 4-6.
[14] S.B. Lyon, R. Bingham, D.J. Mills, Advances in corrosion protection by organic coatings: what we know and what we would like to know, Progr. Org. Coat. 102 (2017) 2–7.
[15] ISO 4287, Geometrical Product Specifications (GPS) - Surface Texture: Profile Method - Terms, Definitions and Surface Texture Parameters, (1997).
[16] ASME B46.1-2009, Surface Texture (Surface Roughness, Waviness, and Lay), American Society of Mechanical Engineers, New York, NY, 2010.
[17] ASTM D4541-17, Standard Test Method for Pull-Off Strength of Coatings Using Portable Adhesion Testers, ASTM International, West Conshohocken, PA, 2017.
[18] B. Persson, M. Scaraggi, Theory of adhesion: role of surface roughness, J. Chem. Phys. 141 (2014) 124701.
[19] S. Pletincx, L.L.I. Fockaert, J.M.C. Mol, T. Hauffman, H. Terryn, Probing the formation and degradation of chemical interactions from model molecule/metal oxide to buried polymer/metal oxide interfaces, Npj Mater. Degrad. 3 (2019) 23.
[20] J. Simão, D.K. Aspinwall, M.L.H. Wise, M.F. EI-Menshawy, Mill roll texturing using EDT, J. Mater. Process. Technol. 45 (1994) 207–214.
[21] S.G. Croll, S.A. Payne, Quantifying abrasive-blasted surface roughness profiles using scanning electron microscopy, Accepted for publication in J. Coat. Technol. Res. (2020).
[22] S. Abbott, Adhesion Science Principles and Practice, Destech Publications Inc., Lancaster, PA, 2015.
[23] D. Beamish, Replica tape: unlocking hidden information, JPCL 32 (7) (2015) 51–62.
[24] H.E. Bennett, J.O. Porteus, Relation between surface roughness and specular reflectance at normal incidence, J. Opt. Soc. Am. 51 (2) (1961) 123–129.
[25] R. Leach, Surface topography measurement instrumentation, Chapter 6, in: R. Leach (Ed.), Fundamental Principles of Engineering Nanometrology, 2nd edition, Elsevier, 2014, pp. 133–204.
[26] R. Leach, C. Evans, L. He, A. Davies, A. Duparré, A. Henning, C.W. Jones, D. O'Connor, Open questions in surface topography measurement: a roadmap, Surf. Topogr.: Metrol. Prop. 3 (2015) 013001.
[27] L.F. Richardson, The problem of contiguity; an appendix of statistics of deadly quarrels, Gen. Syst. 6 (1961) 139–187.
[28] E. Bouchard, G. Lapasset, J. Planès, Fractal dimension of fractured surfaces: a universal value? Europhys. Lett. 13 (1) (1990) 73–79.
[29] B.N.J. Persson, On the fractal dimension of rough surfaces, Tribol. Lett. 54 (2014) 99–106.
[30] Q. Ye, B. Shen, O. Tiedje, J. Domnick, Investigations of spray painting processes using an airless spray gun, J. Energy Power Eng. 7 (2013) 74–81.
[31] S. Kooij, R. Sijs, M.M. Denn, E. Villermaux, D. Bonn, What Determines the Drop Size in Sprays? Phys. Rev. X 8 (2018) 031019.
[32] C.K. Schoff, Craters and other coatings defects: mechanisms and analysis, Chapter 18, in: M. Wen, K. Dusek (Eds.), Protective Coatings: Film Formation and Properties, Springer, New York, 2017.
[33] D. Li, D. Zhang, Z. Zheng, Xi Tian, Numerical analysis on air entrapment during a droplet impacts on a dry flat surface, Int. J. Heat Mass Transf. - Theory Appl. 115 (2017) 186–193.
[34] A. Dalilia, S. Chandra, J. Mostaghimi, H.T.C. Fan, J.C. Simmer, Bubble entrapment and escape from sprayed paint films, Prog. Org. Coat. 97 (2016) 153–165.
[35] K.R. Langley, E.Q. Li, I.U. Vakarelski, S.T. Thoroddsen, The air entrapment under a

drop impacting on a nano-rough surface, Soft Matter 14 (2018) 7586–7596.
[36] N.A. de Bruyne, The Extent of Contact Between Glue and Adherend, Aero Research Technical Notes, No. 168, December 1956, Tech. Service Dept., Aero Research Ltd., Dufford, Cambridge, 2020, pp. 1–12.
[37] C.W. Paul, How thermodynamics drives wet-out in adhesive bonding: correcting common misconceptions, J. Adhesion Sci. Technol. 22 (2008) 31–45.
[38] J.W. Gibbs, A method of geometrical representation of the thermodynamic properties of substances by means of surfaces, Trans. Conn. Acad. Arts Sci. vol. ii, (1873) 382–404 Chapter II in The Scientific Papers of J. Willard Gibbs, Longmans, Green and Co.: London, 1906 (Republished by Dover: New York, 1961).
[39] Y. Tsoumpas, S. Dehaeck, M. Galvagno, A. Rednikov, H. Ottevaere, U. Thiele, P. Colinet, Nonequilibrium Gibbs' criterion for completely wetting volatile liquids, Langmuir 30 (2014) 11847–11852.
[40] J.H. Snoeijer, J. Eggers, Asymptotic analysis of the dewetting rim, Phys. Rev. E 82 (2010) 056314.
[41] J. Bico, U. Thiele, D. Quére, Wetting of textured surfaces, Colloids Surf. A Physicochem. Eng. Asp. 206 (2002) 41–46.
[42] G. Kacar, E.A.J.F. Peters, L.G.J. van der Ven, G. de With, Hierarchical multi-scale simulations of adhesion at polymer–metal interfaces: dry and wet conditions, Phys. Chem. Chem. Phys. 17 (2015) 8935.
[43] W. Funke, Thin-layer technology in organic coatings, Prog. Org. Coatings 28 (1996) 3–7.
[44] C. Wehlack, W. Possart, Characterization of the metal-epoxy interphase: FTIR-ERAS and spectra calculation for ultra-thin films, Macromol. Symp. 205 (2004) 251–261.
[45] R. Grayburn, Z.E. Voras, C.M. Goodwin, M.-C. Liu, T.P. Beebe Jr., A. Phenix, Ion probe techniques to measure the distribution of substrate elements in coatings for copper alloys, Prog. Org. Coat. 111 (2017) 267–272.
[46] J. Prousek, Fenton chemistry in biology and medicine, Pure Appl. Chem. 79 (12) (2007) 2325–2338.
[47] M.F. Mecklenburg, C.S. Tumosa, E.P. Vicenzi, The influence of pigments and ion migration on the durability of drying oil and alkyd paints, universidad politecnica de Valencia and Museum conservation institute, New Insights into the Cleaning of Paintings: Proceedings from the Cleaning 2010 International Conference (2010) 59–67.
[48] A. Ammala, S. Bateman, K. Dean, E. Petinakis, P. Sangwan, S. Wong, Q. Yuan, L. Yu, C. Patrick, K.H. Leong, An overview of degradable and biodegradable polyolefins, Prog. Polym. Sci. 36 (2011) 1015–1049.
[49] M.R. Begley, J.W. Hutchinson, The Mechanics and Reliability of Films, Multilayers and Coatings, Cambridge University Press, Cambridge UK, 2017.
[50] A.J. Kinloch, A.J. Kinloch (Ed.), Durability of Structural Adhesives, Applied Science Publishers, London, 1983.
[51] A. Baldan, Review Adhesively-bonded joints and repairs in metallic alloys, polymers and composite materials: adhesives, adhesion theories and surface pretreatment, J. Mater. Sci. 39 (2004) 1–49.
[52] ASTM D3363-05(2011)e2, Standard Test Method for Film Hardness by Pencil Test, ASTM International, West Conshohocken, PA, 2011.
[53] ASTM D3359-17, Standard Test Methods for Rating Adhesion by Tape Test, ASTM International, West Conshohocken, PA, 2017.
[54] K.L. DeVries, D.O. Adams, Mechanical testing of adhesive joints, Chapter 6, in: D.A. Dillard, A.V. Pocius (Eds.), The Mechanics of Adhesion, Elsevier, 2002.
[55] S.G. Croll, C. Siripirom, B.D. Keil, Finite element analysis to locate maximum values of the first and second principal strains in the tensile pull-off test for coating adhesion on large pipes, Proceedings SSPC 2014, 10-13th February 2014, Orlando Florida, 2014.
[56] S.G. Croll, B.D. Keil, Adhesion measurements of coatings on cylindrical steel pipes: variability & significance, Proceedings SSPC 2014, 10-13th February 2014, Orlando Florida, 2014.
[57] K. Kendall, Energy analysis of adhesion, Chapter 3, in: D. Dillard, A.V. Pocius (Eds.), The Mechanics of Adhesion, Elsevier, 2002, pp. 77–110.
[58] A.N. Gent, A.J. Kinloch, Adhesion of Viscoelastic Materials to Rigid Substrates. III. Energy Criterion for Failure, J. Polym. Sci. Part A-2 Polym. Phys. (9) (1971) 659–668.
[59] D.E. Packham, Surface energy, surface topography and adhesion, Int. J. Adhesion Adhesives 23 (2003) 437–448.
[60] E.H. Andrews, A.J. Kinloch, Mechanics of adhesion I, Proc. Roy. Soc., A 332 (1973) 385–399.
[61] C.Y. Hui, D. Xu, E.J. Kramer, A fracture model for a weak interface in a viscoelastic material (small scale yielding analysis), J. Appl. Phys. 72 (1992) 3294–3304.
[62] K.M. Liechti, Fracture mechanics and singularities in bonded systems, Chapter 2, in: D.A. Dillard, A.V. Pocius (Eds.), The Mechanics of Adhesion, Elsevier, 2002, pp. 45–76.
[63] C.H.M. Hagen, O.Ø. Knudsen, A.H. Zavieh, W. Pfleging, Effect of laser structured micro patterns on the polyvinyl butyral/oxide/steel interface stability, Prog. Org. Coatings 147 (2020) 105766.
[64] M.D. Thouless, A.G. Evans, M.F. Ashby, J.W. Hutchinson, The edge cracking and spalling of brittle plates, Acta. metall. 35 (6) (1987) 1333–1341.
[65] A.G. Evans, M. Rohle, B.J. Dalgleish, R.G. Charalambides, The fracture energy of bimaterial interfaces, Mats. Sci. Eng., A126 (1990) 53–64.
[66] A.A. Griffith, The phenomena of rupture and flow in solids, Philos. Trans. Math. Phys. Eng. Sci. 221 (1921) 582–593.
[67] B. Chen, D.A. Dillard, Crack path selection in adhesively bonded joints, Chapter 11, in: D.A. Dillard, A.V. Pocius (Eds.), The Mechanics of Adhesion, Elsevier, 2002, pp. 389–442.
[68] R.J. Asaro, N.P. O'Dowd, C.F. Shih, Elastic-plastic analysis of cracks on bimaterial interfaces: interfaces with structure, Mats Sci Eng., A162 (1993) 175–192.
[69] J.P.B. van Dam, S.T. Abrahami, A. Yilmaz, Y. Gonzalez-Garcia, H. Terryn, J.M.C. Mol, Effect of surface roughness and chemistry on the adhesion and durability of a steel-epoxy adhesive interface, Int. J. Adhesion Adhesives 96 (2020) 102450.
[70] Q.D. Yang, M.D. Thouless, Mixed-mode fracture analyses of plastically-deforming adhesive joints, Int. J. Fract. Mech. 110 (2001) 175–187.
[71] S.G. Croll, Adhesion loss due to internal strain, J. Coat. Technol. Res. 52 (665) (1980) 35–43.
[72] K. Kendall, The adhesion and surface energy of elastic solids, J. Phys. D Appl. Phys. 4 (1971) 1186–1195.
[73] V. Pandey, A. Fleury, R. Villey, C. Creton, M. Ciccotti, Linking peel and tack performances of pressure sensitive adhesives, Soft Matter 16 (2020) 3267–3275.
[74] E. Sancaktar, R. Gomatam, A study on the effects of surface roughness on the strength of single lap joints, J. Adhesion Sci. Technol. 15 (1) (2001) 97–117.
[75] S. Zhang, R. Panat, K.J. Hsia, Influence of surface morphology on the adhesive strength of epoxy-aluminium interfaces, J. Adhesion Sci. Technol 17 (12) (2003) 1685–1711.
[76] V. Janarthanan, P.D. Garrett, R.S. Stein, M. Srinivasarao, Adhesion enhancement in immiscible polymer bilayer using oriented macroscopic roughness, Polymer 38 (l) (1997) 105–111.
[77] J. Liu, M.K. Chaudhury, D.H. Berry, J.E. Seebergh, J.H. Osborne, K.Y. Blohowiak, Effect of surface morphology on crack growth at a sol-gel reinforced Epoxy/Aluminum interface, J. Adhesion 82 (5) (2006) 487–516.
[78] V. Tvergaard, J.W. Hutchinson, The relation between crack growth resistance and fracture process parameters in elastic-plastic solids, J. Mech. Phys. Solids 40 (6) (1992) 1377–1397.
[79] A.G. Evans, J.W. Hutchinson, Effects of non-planarity on the mixed mode fracture resistance of bimaterial interfaces, Acta metall. 37 (3) (1989) 909–916.
[80] J.W. Hutchinson, Z. Suo, Mixed mode cracking in layered structures, J. Adv. Res. Appl. Mech. Comput. Fluid Dyn. 29 (1992) 63–191.
[81] P.D. Zavattieri, L.G. Hector Jr, A.F. Bower, Cohesive zone simulations of crack growth along a rough interface between two elastic–plastic solids, Eng. Fract. Mech. 75 (2008) 4309–4332.
[82] F.A. Cordisco, P.D. Zavattieria, L.G. Hector Jr, B.E. Carlson, Mode I fracture along adhesively bonded sinusoidal interfaces, Int. J. Solids Struct. 83 (2016) 45–64.
[83] K.T. Faber, A.G. Evans, Crack deflection processes – I. Theory, Acta Metallica. 31 (4) (1983) 565–576.
[84] B.-W. Li, H.-P. Zhao, Q.-H. Qin, X.-Q. Feng, S.-W. Yu, Numerical study on the effects of hierarchical wavy interface morphology on fracture toughness, Comput. Mat. Sci. 57 (2012) 14–22.
[85] S. Hariyadi, Y. Munemoto, Sonoda, Experimental Analysis of anchor bolt in concrete under the pull-out loading, Procedia Eng. 171 (2017) 926–933.
[86] S. Yang, Z. Wu, X. Hu, J. Zheng, Theoretical analysis on pullout of anchor from anchor–mortar–concrete anchorage system, Eng. Fract. Mech. 75 (2008) 961–985.
[87] C. Creton, M. Ciccotti, Fracture and adhesion of soft materials: a review, Rep. Prog. Phys. 79 (2016) 046601.
[88] T. Yamaguchi, K. Koike, M. Doi, In situ observation of stereoscopic shapes of cavities in soft adhesives, Eur. Phys. J. E 77 (2007) 64002.
[89] A. Zosel, The effect of fibrilation on the tack of pressure sensitive adhesives, Int. J. Adhesion Adhesives 18 (1998) 365–271.
[90] W. Li, D.Y. Li, Influence of surface morphology on corrosion and electronic behavior, Acta Mater. 54 (2006) 445–452.
[91] N. Bjerrum, Ionic association. I. Influence of ionic association on the activity of ions at moderate degrees of association, Kgl. Danske Videnskab. Selskab. Mathfys. Medd. 9 (7) (1926) 1–48.
[92] D.M. Kroll, S.G. Croll, Heterogeneity in polymer networks formed by a single copolymerization reaction: II. Post-gelation structure and pendants, Polymer 116 (2017) 113–123.
[93] D.J. Yaron, T. Kowalewski, Beware the nanovoids, Nat. Mater. 18 (11) (2019) 1154–1155.
[94] R.A. Gledhill, A.J. Kinloch, Environmental failure of structural adhesive joints, J. Adhesion 6 (4) (1974) 315–330.
[95] J. Comyn, Kinetics and mechanism of environmental attack, Chapter 3, in: A.J. Kinloch (Ed.), Durability of Structural Adhesives, Applied Science Publishers, 1983, pp. 85–131.
[96] I. Linossier, F. Gaillard, M. Romand, T. Nguyen, A spectroscopic technique for studies of water transport along the interface and hydrolytic stability of Polymer/Substrate systems, J. Adhesion 70 (3-4) (1999) 221–239.
[97] A. Nazarov, N. Le Bozec, D. Thierry, Assessment of steel corrosion and deadhesion of epoxy barrier paint by scanning Kelvin probe, Prog. Org. Coat. 114 (2018) 123–134.
[98] J. Wielant, R. Posner, R. Hausbrand, G. Grundmeier, H. Terryn, Cathodic delamination of polyurethane films on oxide covered steel – combined adhesion and interface electrochemical studies, Corros. Sci. 51 (2009) 1664–1670.
[99] P.A. Sørensen, S. Kiil, K. Dam-Johansen, C.E. Weinell, Influence of substrate topography on cathodic delamination of anticorrosive coatings, Prog. Org. Coat. 64 (2009) 142–149.
[100] N.W. Khun, G.S. Frankel, Effects of surface roughness, texture and polymer degradation on cathodic delamination of epoxy coated steel samples, Corros. Sci. 67 (2013) 152–160.
[101] G. Bahlakeh, B. Ramezanzadeh, A detailed molecular dynamics simulation and experimental investigation on the interfacial bonding mechanism of an epoxy adhesive on carbon steel sheets decorated with a novel cerium−Lanthanum nanofilm, ACS appl, Mater. Interfaces 9 (2017) 17536–17551.
[102] W. Fürbeth, M. Stratmann, The delamination of polymeric coatings from electrogalvanized steel - a mechanistic approach. Part 3: delamination kinetics and

influence of CO2, Corr. Sci. 43 (2) (2001) 243–254.
[103] J.A. Boscoboinik, Chemistry in confined space through the eyes of surface science—2D porous materials, J. Phys. Condens. Matter 31 (2019) 063001.
[104] D. Feng, X. Li, X. Wang, J. Li, T. Zhang, Z. Sun, M. He, Q. Liu, J. Qin, S. Han, J. Hu, Anomalous capillary rise under nanoconfinement: a view of molecular kinetic theory, Langmuir 34 (2018) 7714–7725.
[105] P. Bampoulis, K. Sotthewes, E. Dollekamp, B. Poelsema, Water confined in two-dimensions: fundamentals and applications, Surf. Sci. Rep. 73 (2018) 233–264.
[106] H. Leidheiser Jr., W. Wang, L. Igetoft, The mechanism for the cathodic delamination of organic coatings from a metal surface, Prog. Org. Coat. 11 (1983) 19–40.
[107] L. Courbin, J.C. Bird, M. Reyssat, H.A. Stone, Dynamics of wetting: from inertial spreading to viscous imbibition, J. Phys. Condens. Matter 21 (2009) 464127.